

NONLINEAR REGULAR AND CHAOTIC

FLUTTER OF A HELICOPTER

Zbigniew Dźygadło and Grzegorz Kowaleczko

Military University of Technology

ul. Kaliskiego 2, 00-908 Warsaw, Poland

Abstract

A method of the flutter phenomenon analysis is presented in this paper. The analysis has been performed for a one-main rotor helicopter on the basis of a complete set of nonlinear differential equations. This set has been adopted from flight mechanics. Basic equations have been modified by taking into account forces and moments produced by a landing gear. Some selected results of numerical calculations are presented.

Introduction

Numerous investigations of the flutter phenomenon of the helicopter have been made [1]÷[4]. Usually the flutter for an isolated blade has only been investigated. In this paper the complete model of the one-main rotor helicopter has been described. This model has been adopted from flight mechanics. Basically, it was applied for the analysis of flight mechanics problems, for instance, manoeuvres with stall aerodynamics effects or flight in failure of the main rotor blade system.

For the basic analysis it is assumed that the helicopter fuselage is a rigid body and the main rotor consists of four rigid blades which are considered separately. Each blade performs motions about its horizontal flapping hinge and vertical lagging hinge. The tail rotor has been treated as a hingeless and weightless source of thrust, which equilibrates the drag moment and ensures directional control of the helicopter.

The above described model has been modified for flutter and ground resonance phenomena analysis. Following modifications have been performed:

- the motion of rigid blades about the axial hinges has been considered;
- landing gear rigidity and damping have been taken into account.

1. Formulation of the problem

1.1. Systems of coordinates

To determine the mathematical model of a helicopter, the following systems of coordinates are assumed:

$Ox_g y_g z_g$ - a moving coordinate system connected with the earth, $Ox_k y_k z_k$ - a system connected with the fuselage, $P_x'' y'' z''$ - a system connected with an element of the main rotor hub with origin at the centre of hub, $P_{Hi} x'_i y'_i z'_i$ - a system connected with the flapping hinge P_{Hi} of i -th blade with the origin in this hinge, $P_{Vi} x_i y_i z_i$ - a system connected with i -th blade of the main rotor with the origin in the lagging hinge P_{Vi} of the blade.

All these systems are shown in Fig.1.1 and they are described in details in [11].

Systems $Ox_g y_g z_g$ and $Ox_k y_k z_k$ are interconnected by the angles of yaw Ψ , pitch Θ and roll Φ . The relation between them has the form:

$$\bar{X}_k = \hat{\alpha} \bar{X}_g \quad (1.1)$$

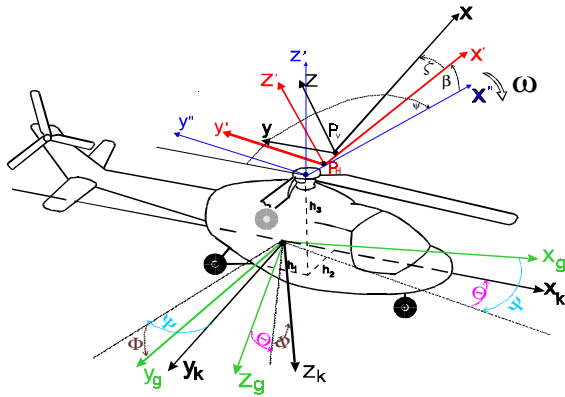


Fig.1.1 Physical model of the helicopter and coordinate systems

As regards $Ox_k y_k z_k$ and $P_{Vi} x_i y_i z_i$ systems, they are interconnected by the angle ψ_i , which is that of azimuth of the i -th blade as measured from the tail boom in the sense of rotation of the main rotor, the angle β_i which is that of flapping of the i -th blade about the horizontal hinge and the angle ζ_i which is that of lagging of the i -th blade about the vertical hinge. This relation has the form:

$$\bar{X} = \hat{\gamma}_i \bar{X}_k \quad (1.2)$$

The analogous relation between $Ox_k y_k z_k$ and $P_{Hi} x_i y_i z_i$ is:

$$\bar{X}' = \hat{\gamma}'_i \bar{X}_k \quad (1.3)$$

Matrix $\hat{\gamma}'_i$ is obtained from matrix $\hat{\gamma}_i$ by substitution $\zeta_i = 0$.

The systems $Ox_k y_k z_k$ and $P_X'' y'' z''$ are interconnected by azimuth ψ . The relation has the form:

$$\bar{X}'' = \hat{\gamma}'' \bar{X}_k \quad (1.4)$$

Matrix $\hat{\gamma}'_i$ is obtained from matrix $\hat{\gamma}_i$ by substitution $\zeta_i = 0$ and $\beta_i = 0$.

1.2. Determination of the equations of motion

The equations of motion have been derived on the basis of Newton's second law of dynamics. They have been applied separately for the fuselage, elements of each blade, elements of each connector and elements of the hub. On the basis of these equations the following equations have been obtained:

1. Equations of translatory motion of the helicopter:

$$M_k \frac{dV_c}{dt} + \sum_{i=1}^k \int_{P_{Vi}}^R \bar{W}_i dm_i + \sum_{i=1}^k \int_{P_{Hi}}^{P_{Vi}} \bar{W}'_i dm'_i + \iiint_V \bar{W}'' dm'' = \bar{F} + \bar{T} + \bar{T}_{tr} \quad (1.5)$$

where: M_k is the mass of the fuselage, V_c - the velocity of the fuselage mass centre, \bar{W}_i , \bar{W}'_i , \bar{W}''_i - the absolute accelerations of the i -th blade element, the i -th connector element and the hub element respectively, \bar{F} - the vector of external forces acting on the fuselage, \bar{T}_{tr} - the thrust of tail rotor.

\bar{T} - the vector of external forces acting on the rotor:

$$\bar{T} = \sum_{i=1}^k \int_{P_{Vi}}^{BR} \bar{q}_i dr_i + \sum_{i=1}^k \int_{P_{Hi}}^{P_{Vi}} \bar{q}'_i dr'_i + \iiint_V d\bar{F}'' \quad (1.6)$$

"B" is the tip-loss factor, $\bar{q}_i dr_i$, $\bar{q}'_i dr'_i$, $d\bar{F}''$ - represent vectors of external forces acting on the

i -th blade element, the i -th connector element and the hub element respectively.

2. The equation of equilibrium of moments about the centre of mass of the fuselage:

$$\frac{d\bar{K}}{dt} + \sum_{i=1}^k \int_{P_{Vi}}^R \bar{R}_i \times \bar{W}_i dm_i + \sum_{i=1}^k \int_{P_{Hi}}^{P_{Vi}} \bar{R}'_i \times \bar{W}'_i dm'_i + \iiint_V \bar{R}'' \times \bar{W}'' dm'' = \bar{M} + \bar{M}_T + \bar{M}_{tr} \quad (1.7)$$

where: \bar{R}_i , \bar{R}'_i , \bar{R}'' are the vectors which determine respectively the location of the i -th blade element, the i -th connector element and the hub element with reference to the centre of mass of the fuselage /Fig.1.2/.

$$\bar{M}_T = \sum_{i=1}^k \int_{P_{Vi}}^{BR} \bar{R}_i \times \bar{q}_i dr_i + \sum_{i=1}^k \int_{P_{Hi}}^{P_{Vi}} \bar{R}'_i \times \bar{q}'_i dr'_i + \iiint_V \bar{R}'' \times d\bar{F}'' \quad (1.8)$$

is the moment of external forces about the centre of mass of the fuselage.

3. The equation describing rotation motion of the main rotor around the axis of the hub:

$$\sum_{i=1}^k \int_{P_{Vi}}^R [(\bar{l}_{Hi} + \bar{l}_{Vi} + \bar{r}_i) \times \bar{W}_i dm_i]_z + \sum_{i=1}^k \int_{P_{Hi}}^{P_{Vi}} [(\bar{l}_{Hi} + \bar{r}'_i) \times \bar{W}'_i dm'_i]_z + \iiint_V [r'' \times \bar{W}'' dm'']_z = [\bar{M}_p]_z + [\bar{M}_{rk}]_z \quad (1.9)$$

where \bar{M}_{rk} is the reaction moment of the fuselage which is at normal flow conditions equal to the moment of the power system; \bar{M}_p is the moment of external forces with reference to the centre of the hub P . Its projection on the Pz'' is determined by the relation:

$$\begin{aligned} [\bar{M}_p]_{z''} = & \sum_{i=1}^k \int_{R_{Vi}}^{BR} [(\bar{l}_{Hi} + \bar{l}_{Vi} + \bar{r}_i) \times \bar{q}_i dr_i]_{z''} + \\ & + \sum_{i=1}^k \int_P^{R_{Vi}} [(\bar{l}_{Hi} + \bar{r}_i) \times \bar{q}_i' dr_i']_{z''} + \oint_V [r'' \times dF'']_{z''} \end{aligned} \quad (1.10)$$

4. The equation of equilibrium of the moments of forces acting on a blade about the flapping hinge P_H :

$$\begin{aligned} & \int_{R_{Vi}}^R [(\bar{l}_{Vi} + \bar{r}_i) \times \bar{W}_i dm_i]_{y_i} + \\ & + \int_{P_{Hi}}^{R_{Vi}} [\bar{r}_i' \times \bar{W}_i' dm_i']_{y_i} = [\bar{M}_{P_{Hi}}]_{y_i} + [\bar{M}_\beta]_{y_i} \end{aligned} \quad (1.11)$$

Lower index $[]_{y_i}$ indicates a projection on the axis $P_{Hi}y_i$ of this hinge; $[\bar{M}_{P_{Hi}}]_{y_i}$ is the external moment acting on the blade about the axis $P_{Hi}y_i$ of hinge P_H :

$$\begin{aligned} [\bar{M}_{P_{Hi}}]_{y_i} = & \int_{R_{Vi}}^{BR} [(\bar{l}_{Vi} + \bar{r}_i) \times \bar{q}_i dr_i]_{y_i} + \\ & + \int_{P_{Hi}}^{R_{Vi}} [\bar{r}_i' \times \bar{q}_i' dr_i']_{y_i} \end{aligned} \quad (1.12)$$

and $[\bar{M}_\beta]_{y_i}$ is the sum of damping and spring moments of the flapping hinge: $\bar{M}_{y_i} = -c_\beta \beta_i - k_\beta \beta_i$

5. The equation of equilibrium of moments of forces acting on a blade about the lagging hinge P_V :

$$\int_{R_{Vi}}^R [\bar{r}_i \times \bar{W}_i dm_i]_{z_i} = [\bar{M}_{R_{Vi}}]_{z_i} + [\bar{M}_\zeta]_{z_i} \quad (1.13)$$

Lower index $[]_{z_i}$ indicates a projection on the axis $P_{Vi}z_i$ of this hinge; $[\bar{M}_{R_{Vi}}]_{z_i}$ is the external moment acting on the blade about the axis $P_{Vi}z_i$ of hinge P_V :

$$[\bar{M}_{R_{Vi}}]_{z_i} = \int_{R_{Vi}}^{BR} [\bar{r}_i \times \bar{q}_i dr_i]_{z_i} \quad (1.14)$$

and $[\bar{M}_\zeta]_{z_i}$ is the sum of damping and spring moments of the lagging hinge: $[\bar{M}_\zeta]_{z_i} = -c_\zeta \zeta_i - k_\zeta \zeta_i$.

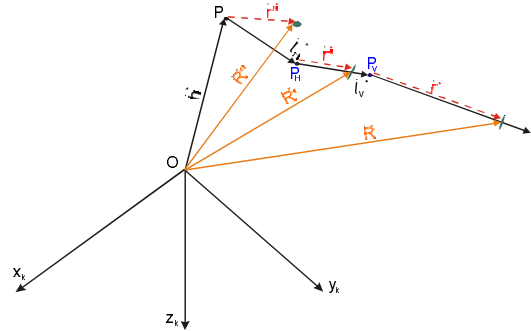


Fig.1.2 Determination of location of blade, connector and hub element

These equations completed with:

- the kinematic relations:

$$\begin{aligned} \dot{\Theta} &= Q \cos \Phi - R \sin \Phi \\ \dot{\Phi} &= P + (Q \sin \Phi + R \cos \Phi) / g \Theta \\ \dot{\Psi} &= (Q \sin \Phi + R \cos \Phi) / \cos \Theta \end{aligned} \quad (1.15)$$
- the relations determining coordinates of the mass centre in the system $Ox_k y_k z_k$:

$$\begin{aligned} x_g &= Ua_{11} + Va_{21} + Wa_{31} \\ y_g &= Ua_{12} + Va_{22} + Wa_{32} \\ z_g &= Ua_{13} + Va_{23} + Wa_{33} \end{aligned} \quad (1.16)$$

and

$$\frac{d\beta_i}{dt} = \dot{\beta}_i, \quad \frac{d\zeta_i}{dt} = \dot{\zeta}_i, \quad \frac{d\psi}{dt} = \omega \quad (1.17)$$

have constituted a set of $14+4k$ nonlinear differential equations with periodic coefficients, where k is a number of blades of the main rotor. They can be expressed in the form:

$$\mathbf{A}^*(t, \bar{X}^*) \bar{X}^* + \mathbf{B}(t, \bar{X}^*) = \bar{f}^*(t, \bar{X}^*, \bar{S}) \quad (1.18)$$

where \bar{X}^* is the vector of flight parameters:

$$\bar{X}^* = (U, V, W, P, Q, R, \omega, \beta_i, \zeta_i, \beta_i, \zeta_i, \psi, \Theta, \Phi, \Psi, x_g, y_g, z_g)^T$$

and U, V, W are linear velocities of the centre of fuselage mass in the coordinate system $Ox_k y_k z_k$ fixed with the fuselage, P, Q, R are angular velocities of the fuselage in the same coordinate system, Θ, Φ, Ψ are the pitch, the roll and the

yaw angles of the fuselage, β_i - the i -th blade flapping rotation about horizontal hinge P_H , ζ_i - the i -th blade lagging rotation about vertical hinge P_V , ω - the angular velocity of the main rotor, ψ - the azimuth of the main rotor.

A vector \bar{S} is the vector of control parameters:

$$\bar{S} = (\theta_0, \kappa_s, \eta_s, \varphi_{so})^T$$

where: θ_0 is the angle of collective pitch of the main rotor, κ_s is the control angle in the longitudinal motion, η_s is the control angle in the lateral motion and φ_{so} is the angle of collective pitch of the tail rotor.

The detailed way of determining the set (1.18) is shown in [11]. For the determination of matrix A and vector \bar{B} there were successively established: the locations of all helicopter elements, the absolute velocities of these elements and their absolute accelerations.

The feathering motions of blades have not been included in the set (1.18). For analysis of flutter it is necessary to take into account these motions and all couplings /particularly between feathering and flapping/. Because of that, the above described model of a helicopter has been modified by assuming that all rigid blades perform motions about their axial hinges /feathering motions/. Equations describing self-coupled flapping and feathering motions have been taken from [1], and [10]. They have the following form:

$$C(t, \bar{Y})\bar{Y} + \bar{D}(t, \bar{Y}) = \bar{g}(t, \bar{Y}, \bar{S}) \quad (1.19)$$

where $\bar{Y} = (\beta_i, \dot{\beta}_i, \phi_i, \dot{\phi}_i)^T$. ϕ_i is a feathering angle of the i -th blade.

On the basis of Eqs. (1.18) and (1.19), a set of 38 nonlinear differential equations has been obtained ($k=4$):

$$\mathbf{A}(t, \bar{X})\bar{X} + \mathbf{B}(t, \bar{X}) = \bar{f}(t, \bar{X}, \bar{S}) \quad (1.20)$$

where \bar{X} is the vector of flight parameters:

$$\bar{X} = (U, V, W, P, Q, R, \omega, \beta_i, \zeta_i, \dot{\beta}_i, \dot{\zeta}_i, \phi_i, \dot{\phi}_i, \psi, \Theta, \Phi, \Psi, x_g, y_g, z_g)^T$$

2. Forces and moments acting on a helicopter

The vector $\bar{f}(t, \bar{X}, \bar{S})$ on the right hand side of equation (1.20) determines external forces

and moments acting on a helicopter and on its parts and represents also right hand sides of equations (1.15) ÷(1.17). These forces and moments may be divided into three groups: 1. the aerodynamic forces and moments; 2. the gravitation forces and moments; 3. the forces and moments produced by the landing gear.

Detailed method of determining all these forces and moments is presented in [11]. In this paper only the main features of this method are described.

2.1 Aerodynamic forces

The aerodynamic forces and moments acting on the rotor blades have been determined making use of static characteristics of the airfoil. Because of specific flow conditions of the blade airfoil (wide range of the angles of attack, reverse flow) /cf. [8]/ these characteristics have been determined for the full range of the angles of attack for different Mach numbers:

$$C_{xa} = C_{xa}(\alpha, Ma) \quad (2.1)$$

$$C_{za} = C_{za}(\alpha, Ma) \quad (2.2)$$

The applied aerodynamic static characteristics of the NACA 23012 airfoil for Mach numbers from 0.3 to 0.8 for the full range of angles of attack have been taken from [5]. They are shown in Figs. 2.1 and 2.2.

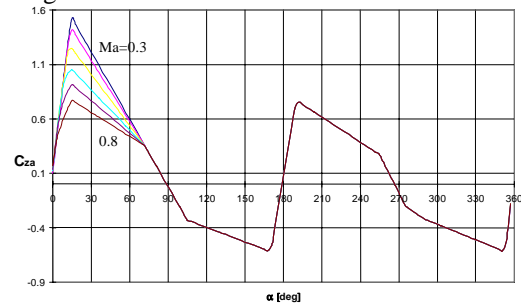


Fig.2.1 The lift coefficient of the airfoil NACA 23012

Components of aerodynamic forces have been determined for each airfoil /Fig.2.3/:

$$dP_{za} = C_{za} \frac{\rho V^2}{2} b(r) \quad (2.3)$$

$$dP_{xa} = C_{xa} \frac{\rho V^2}{2} b(r) \quad (2.4)$$

where $b(r)$ is an aerodynamic chord of the blade airfoil.

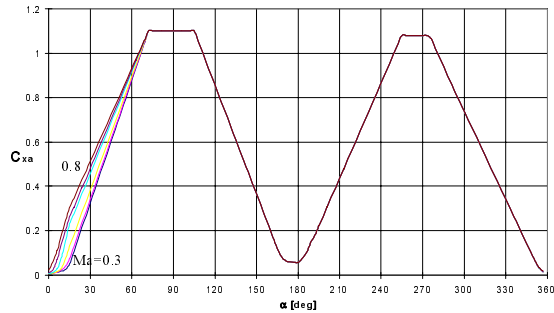


Fig. 2.2 The drag coefficient of the airfoil NACA 23012

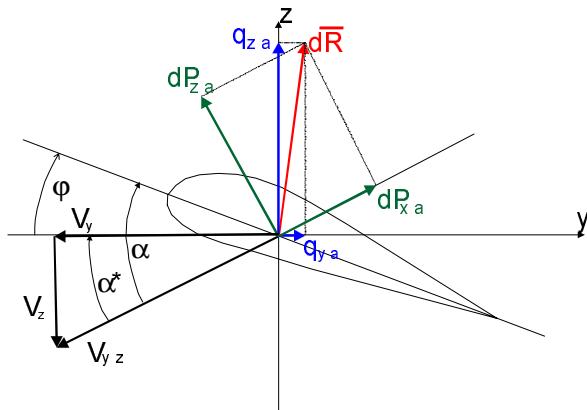


Fig.2.3. Aerodynamic loads of the main rotor blade element

Specific flow conditions of the main rotor blades, even in a steady flight, /motion about hinges, changeability of air velocity flowing around airfoils depending on the blade azimuth, the reverse flow region/ cause that the section incidence α changes within a wide range. The critical angle of attack is often dynamically exceeded. This phenomenon is particularly visible for “retreating “ blades near to the airscrew hub axis of rotation. The region within which the angle of stall is exceeded becomes larger when the speed of flight increases.

In purpose to include into account changes of static characteristics due the airfoil pitching /nonstationary effects/, the method proposed by Tarzanin has been applied ([6], [7]). The example dependence of the lift coefficient, on dynamic stall effects taken into consideration, is presented in Fig. 2.4.

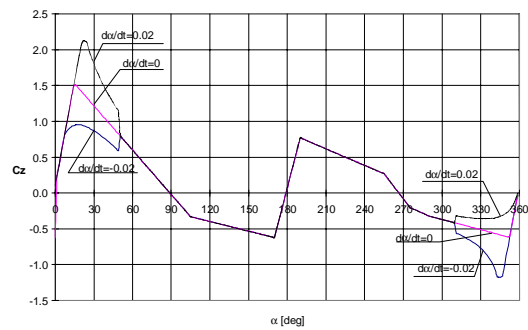


Fig. 2.4 Dynamic stall influence on $C_{za}(\alpha, Ma)$

Because of changes of the blade azimuth the sweep angle of the stream Λ varies /Fig.2.5/. This effect of spanwise (radial) flow on the lift coefficient has also been taken into account. It was performed according to the method described in [6], [7].

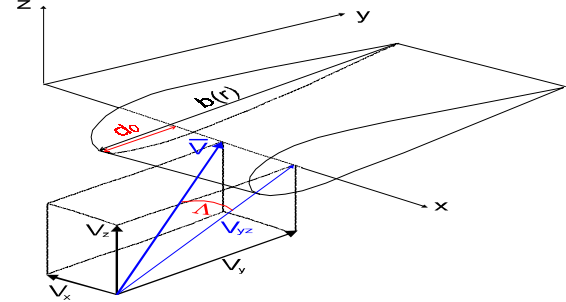


Fig. 2.5 Determination of the sweep angle Λ of the air stream flowing around the blade element

All the aerodynamic forces and moments acting on blades have been calculated by numerical integration along each blade. The induced velocity of each airfoil has been determined by means of Biot-Savart law – four separated strings of vortex have been investigated.

Aerodynamic forces and moments of the fuselage have been calculated on the basis of its experimental aerodynamic characteristics.

2.2. Landing gear forces and moments

In the present case the flutter phenomenon for the helicopter staying on the ground has been investigated. For that reason the landing gear rigidity and damping have been taken into account. All forces and moments produced by the landing gear have been included into the right hand side of Eq. (1.20). It has been assumed that the landing gear consists of three wheels. Configuration of the

landing gear is shown in Fig.1.1. For each wheel its rigidity, damping and position have been determined separately.

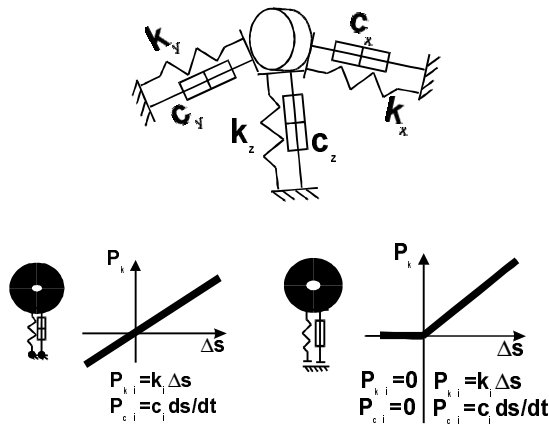


Fig.2.9 Linear and nonlinear models of the landing gear

Two models of landing gear forces have been used /Fig. 2.9/. The first one, where relations between forces and displacement and velocity are linear:

$$\bar{P}_{lg i} = \bar{P}_{ki} + \bar{P}_{ci} \quad (2.5)$$

and the second model where these relations are nonlinear – for the case where there is no contact between wheel and the ground. In this case all forces and moments produced by this wheel are equal to zero:

$$\bar{P}_{lg i} = \begin{cases} \bar{P}_{ki} + \bar{P}_{ci} & \text{for } \Delta h_i < 0 \\ 0 & \text{for } \Delta h_i \geq 0 \end{cases} \quad (2.6)$$

where “ i ” is the number of wheel / $i=1,2,3$ / and Δh_i is the distance between the wheel and the ground.

Components of the force $\bar{P}_{lg i}$ produced by the i -th wheel are equal to:

$$\begin{aligned} X_{lg i} &= -k_{xi} \Delta x_i - c_{xi} \dot{x}_i \\ Y_{lg i} &= -k_{yi} \Delta y_i - c_{yi} \dot{y}_i \\ Z_{lg i} &= -k_{zi} \Delta z_i - c_{zi} \dot{z}_i \end{aligned} \quad (2.7)$$

where k_{xi} , k_{yi} , k_{zi} are stiffness coefficients of the i -th wheel; c_{xi} , c_{yi} , c_{zi} are its damping coefficients; Δx_i , Δy_i , Δz_i are displacements of the “contact point” determined in the system $Ox_k y_k z_k$.

The moment produced by the i -th wheel is equal to:

$$\bar{M}_{lg i} = \bar{R}_{lg i} \times \bar{P}_{lg i} \quad (2.8)$$

where $\bar{R}_{lg i} = (x_{lg i}, y_{lg i}, z_{lg i})$ is the vector determining the location of the i -th wheel with reference to the mass centre of the fuselage. It has the following components:

$$\begin{aligned} L_{lg i} &= Z_{lg i} y_{lg i} - Y_{lg i} z_{lg i} \\ M_{lg i} &= X_{lg i} z_{lg i} - Z_{lg i} x_{lg i} \\ N_{lg i} &= Y_{lg i} x_{lg i} - X_{lg i} y_{lg i} \end{aligned} \quad (2.9)$$

Finally, forces end moments produced by the landing gear are equal to:

$$X_{lg} = \sum_{i=1}^3 X_{lg i}, \quad Y_{lg} = \sum_{i=1}^3 Y_{lg i}, \quad Z_{lg} = \sum_{i=1}^3 Z_{lg i} \quad (2.10)$$

$$L_{lg} = \sum_{i=1}^3 L_{lg i}, \quad M_{lg} = \sum_{i=1}^3 M_{lg i}, \quad N_{lg} = \sum_{i=1}^3 N_{lg i} \quad (2.11)$$

2.3. The thrust of the tail rotor

As it has been stated at the beginning, the tail rotor is treated as the hingeless and weightless source of thrust which equilibrates the drag moment and ensures (in flight dynamics problems) directional control of the helicopter. According to this assumption, the thrust of the tail rotor has been calculated on the basis of the initial value of the drag moment M_{p0} /Eq.(1.10)/. Making use of this value and values of coordinates x_{tr} and z_{tr} / $y_{tr} = 0$ /, determining the location of the tail rotor with reference to the fuselage mass centre one can obtain:

- the thrust of tail rotor:

$$T_{tr} = \frac{M_{p0}}{x_{tr}} \quad (2.12)$$

- the rolling and yawing moments produced by the tail rotor:

$$L_{tr} = -T_{tr} z_{tr}, \quad N_{tr} = -T_{tr} x_{tr} \quad (2.13)$$

3. Solution of the problem

As it was mentioned above, in the present case, the flutter phenomenon for the helicopter staying on the ground has been investigated. The numerical simulations have been performed according to results of experiments performed for a Polish „Sokol” helicopter. During these experiments, the flutter was excited by changing the displacements of the mass centre of the blade

airfoil. The flutter phenomenon was simulated in the same way .

The numerical analysis was based on the set of Eqs.(1.20). Some results of computation are presented in this paper. For all presented cases the initial position of the helicopter has been disturbed /particularly position of the second blade/.

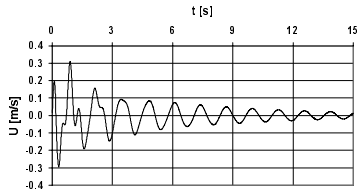


Fig.3.1.1 Linear velocity $U(t)$

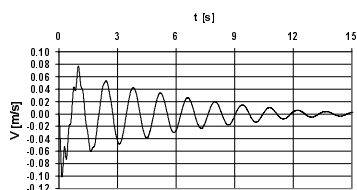


Fig.3.1.2 Linear velocity $V(t)$

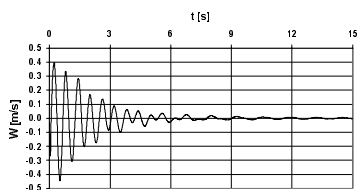


Fig.3.1.3 Linear velocity $W(t)$

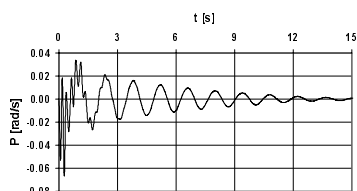


Fig.3.1.4 Angular rolling velocity $P(t)$

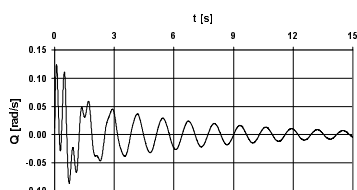


Fig.3.1.5 Angular pitching velocity $Q(t)$

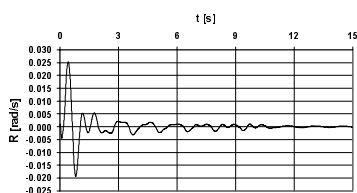


Fig.3.1.6 Angular yawing velocity $R(t)$

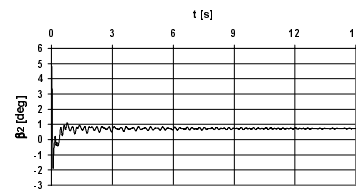


Fig.3.1.7 Flapping of the second blade $\beta_2(t)$

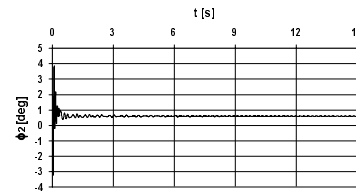


Fig.3.1.8 Feathering of the second blade $\phi_2(t)$

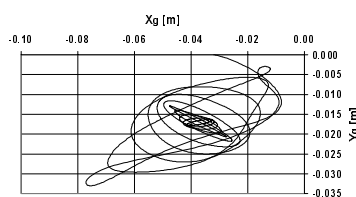


Fig.3.1.9 Trajectory of the fuselage mass centre on $Ox_g y_g$ plane

In the first set of figures /Figs.3.1.1 ÷ 3.1.9/ selected parameters of helicopter motion are shown. One can see that all courses are damped. Of course this means that helicopter is stable and no instability can occur. Because only collective pitch of the main rotor θ_0 is not equal to zero, it is seen that damped oscillations of blades occur. Trajectory of the centre of fuselage mass converges to the point of stability.

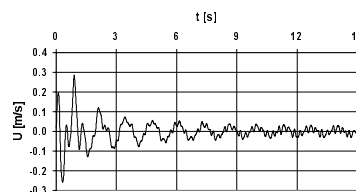


Fig.3.2.1 Linear velocity $U(t)$

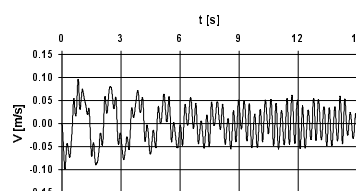


Fig.3.2.2 Linear velocity $V(t)$

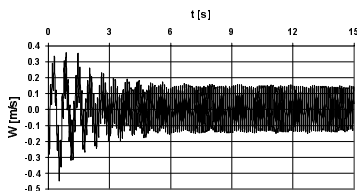


Fig.3.2.3 Linear velocity $W(t)$

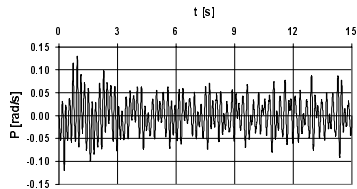


Fig.3.2.4 Angular rolling velocity $P(t)$

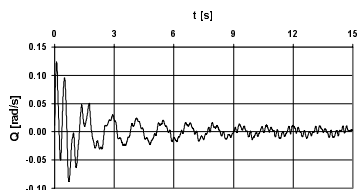


Fig.3.2.5 Angular pitching velocity $Q(t)$

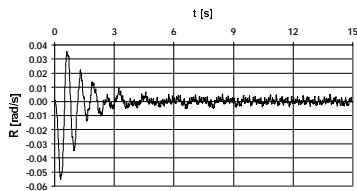


Fig.3.2.6 Angular yawing velocity $R(t)$

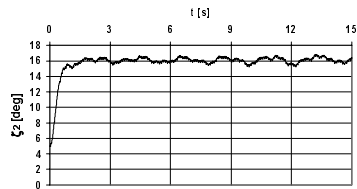


Fig.3.2.7 Lagging of the second blade $\xi_2(t)$

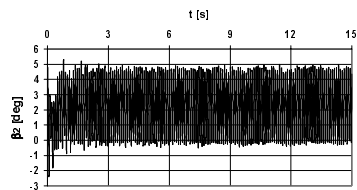


Fig.3.2.8 Flapping of the second blade $\beta_2(t)$

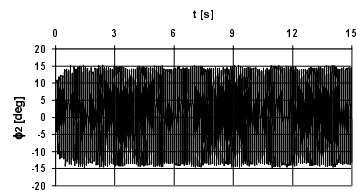


Fig.3.2.9 Feathering of the second blade $\phi_2(t)$

In Figs.3.2.1 ÷ 3.2.9 one can observe that flapping and feathering oscillations don't increase and they have almost constant amplitude. This is typical for non-linear motions. The area of these oscillations is quite wide – particularly for feathering. Because of that the lagging angle of blade is changed – the average value of the drag coefficient increases. We can also see that the rest of parameters change because of couplings between all motions.

In the last figures /Figs.3.3.1 ÷ 3.3.6/ some results of harmonic analysis are presented for courses obtained for flutter simulation. All diagrams have been made according to [12] by Schuster. Those pictures show power spectrums obtained for the helicopter motion. From comparison of our results with those presented by Schuster a conclusion could be drawn that the motion of the helicopter is chaotic.

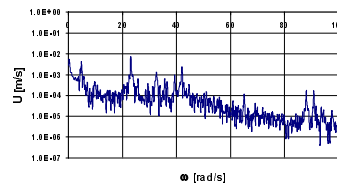


Fig.3.3.1 Linear velocity $U(t)$

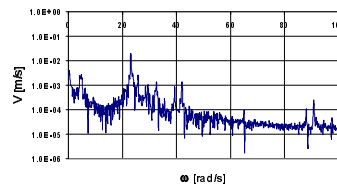


Fig.3.3.2 Linear velocity $V(t)$

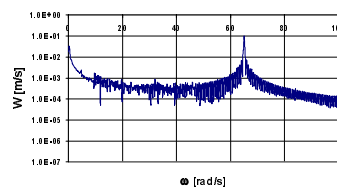


Fig.3.3.3 Linear velocity $W(t)$

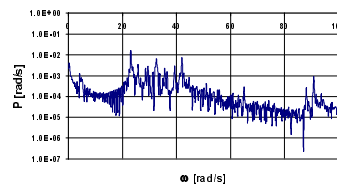


Fig.3.3.4 Angular rolling velocity $P(t)$

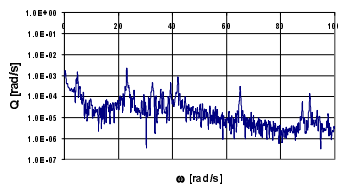


Fig.3.3.5 Angular pitching velocity $Q(t)$

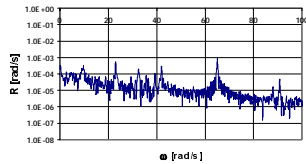


Fig.3.3.6 Angular yawing velocity $R(t)$

4. Concluding remarks

This paper presents the method of the flutter phenomenon analysis for the helicopter treated as the system, which consists of the fuselage and four rigid blades. The complete set of nonlinear differential equations, which describes flutter oscillations of a one-main rotor helicopter, has been obtained. This set enabled us to study the helicopter fuselage motion and motions of all the blades of the main rotor motions. A numerical analysis of the system dynamics has been performed and some results are given in the paper. These results show time histories for various helicopter motion parameters. On the basis of the obtained results we can conclude that the applied model of the one-main rotor helicopter enables more precise study of physical phenomena, which can occur in the real simulations.

Making use of the model a further more detailed analysis of the flutter will be performed. The case of the flutter phenomenon during flight will be included in that analysis.

References

1. Scanlan R., Rosenbaum R., *Introduction to Study of Aircraft Vibration and Flutter*, The Macmillan Company, USA, 1951
2. Ham Norman D., *An experimental investigation of stall flutter*, Journal of the American Helicopter Society, vol. 7/1, 1962

3. Shipman K., Wood E., *A Two-Dimensional Theory for Rotor Blade Flutter in Forward Flight*, Journal of Aircraft, vol. 8/12, 1971
4. Crimi P., *Analysis of Helicopter Rotor Blade Stall Flutter*, Journal of Aircraft, vol. 11/7, 1974
5. Mil M., *Helicopters*, Masinstrojenje, Moscow, 1967 (in Russian)
6. Harris F., Tarzanin F., *Rotor High Speed Performance, Theory vs. Test*, Journal of the American Helicopter Society, vol. 15/32, 1970
7. Tarzanin F., *Prediction of Control Loads Due to Blade Stall*, The Annual National V/STOL Forum of the American Helicopter Society, Washington, 1971
8. Bramwell A., *Helicopter Dynamics*, Edward Arnold Publishers Ltd., London, 1976
9. Ormison R., *Rotor-Fuselage Dynamics of Helicopter Air and Ground Resonance*, Journal of the American Helicopter Society, vol. 36/2, 1991
10. Szabelski K., *Introduction to Design of Helicopters*, Wydawnictwa Komunikacji i Łączności, Warsaw, 1995, (in Polish)
11. Kowaleczko G., *Nonlinear Dynamics of Spatial Motion of a Helicopter*, Military University of Technology, Warsaw, 1998, (in Polish)
12. Schuster H.G., *Deterministic Chaos. An Introduction*, VCH Verlagsgesellschaft, Weinheim, 1988